# Optical Survey of the Tumble Rates of Retired GEO Satellites

**Christopher R. Binz**
**Mark A. Davis***
**Bernie E. Kelm**
**Christopher I. Moore**
*U.S. Naval Research Laboratory, Washington, D.C., 20375*

## 1. ABSTRACT

The Naval Research Lab (NRL) and the Defense Advanced Research Projects Agency (DARPA) have made significant progress toward robotic rendezvous and docking between spacecraft, however the long-term attitude motion evolution of uncontrolled resident space objects has never been well-characterized. This effort set out to identify the motion exhibited in retired satellites at or near geosynchronous orbit (GEO). Through analysis of the periodic structure of observed reflected light curves, estimated tumble rates were determined for several retired satellites, typically in a super-GEO disposal orbit. The NRL's 1-meter telescope at Midway Research Center was used to track and observe the objects while the sun-satellite-observer geometry was most favorable; typically over a one- to two-hour period, repeated multiple times over the course of weeks. By processing each image with calibration exposures, the relative apparent magnitude of the brightness of the object over time was determined. Several tools, including software developed internally, were used for frequency analysis of the brightness curves. Results show that observed satellites generally exhibit a tumble rate well below the notional bounding case of one degree per second. When harmonics are found to exist in the data, modeling and simulation of the optical characteristics of the satellite can help to resolve ambiguities. This process was validated on spacecraft for which an attitude history is known, and agreement was found.

## 2. INTRODUCTION

The behavior of geosynchronous satellites that have been retired and boosted to their disposal orbit in the "graveyard" has long been of interest to the space community.[7, 12, 9, 13] However, the Defense Advanced Research Projects Agency (DARPA) Phoenix[2, 3, 14] mission is one of the first programs for which there is operationally-relevant interest. Several characteristics are of specific interest to Phoenix, and in this paper we address the residual attitude rate properties (i.e. the tumble rates) of these objects.

Phoenix is a DARPA program aimed at developing technologies for more flexible, cost-effective satellite operations in GEO. One of the primary technical areas of research for Phoenix is the development of a variety of robotics technologies to address key on-orbit mission needs, including repositioning, repair, asset life extension, and inspection. These technologies would be part of a future robotic servicing vehicle. It represents a continuation of over a decade of space robotics development by NRL and DARPA[6].

The tumble rate of the asset to be serviced directly impacts trajectory design for the rendezvous and docking phase of the mission, which influences the rate of propellant utilization for the Servicer/Tender. In order to provide a solid basis from which requirements may be derived, the task of providing definitive bounding tumble rates for objects that fit the profile of a potential asset was undertaken.

In setting out to place bounds on the tumble rates found among retired GEO assets, we quickly found that there was only conflicting anecdotal evidence concerning these rates. Thus, began our own survey, using a number of standard tools, in order to independently get a preliminary picture of retired assets that might be of interest to the program.

Due to the great distances involved, all analysis must be performed with unresolved imagery, i.e. light reflected from spacecraft surfaces, with no ability to distinguish any spacecraft features. For this study,

This research was developed with funding from the Defense Advanced Research Projects Agency (DARPA).
*Mark Davis is deceased, and is included as a coauthor for his invaluable contributions to this work.

the telescope at the U.S. Naval Research Laboratory's (NRL) Midway Research Center was used—details are presented in Section 3. As such, the angle between the observer, satellite, and sun is a critical factor in obtaining observations (see Fig. 1). When the geometry is favorable, incident sunlight will be reflected off the various facets of the satellite towards the observer, allowing for measurements of relative brightness magnitude. Of course, observations are only possible when the satellite is not in the Earth's shadow.

The main factors affecting visual observations include atmospheric distortion and the observation geometry. Typically, atmospheric effects may be compensated for by calibrating the measurements against a set of stars for which visual magnitude is well-defined. In this work, the Landolt photometric standards are used—more detail is given in Section 3.[10] Visual magnitude is usually brightest when the Sun-satellite-observer angle is smallest, and it will decrease as this angle grows. Fig. 2 shows how this geometry changes over a given pass.

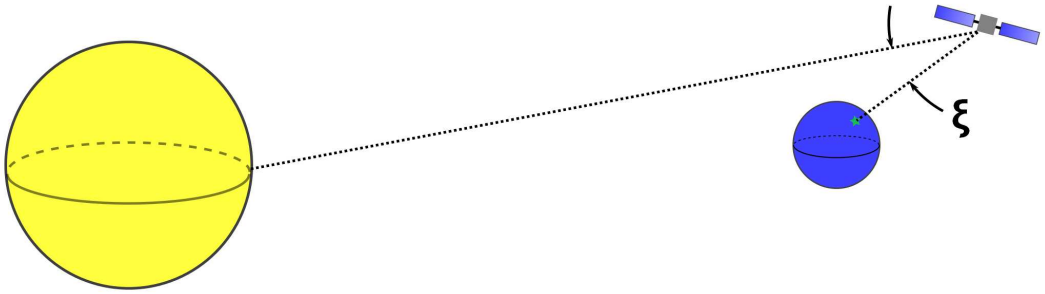


Fig. 1: Sketch showing the observation geometry (not to scale). The Sun is represented in yellow, the Earth in blue, and the observing station is located on Earth's surface.

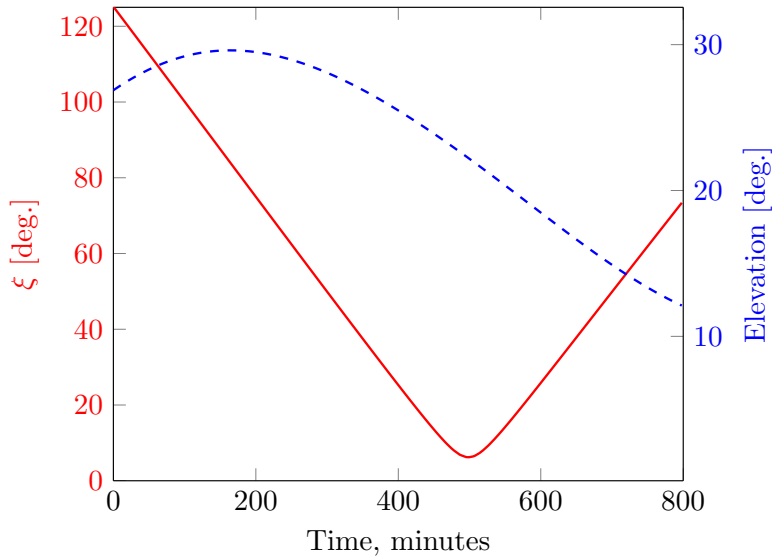


Fig. 2: Plot of the Sun-spacecraft-observer angle $\xi$ and elevation for a typical pass of a retired GEO satellite in a graveyard orbit.

Due to the fact that the objects we are interested in are typically located in a super-GEO disposal orbit, there is a some motion of the spacecraft with respect to the ground. In this study, the telescope was used in *ephemeris tracking* mode,[9] in which the telescope tracks the moving satellite, while stars appear as streaks. This is accomplished with a tracking mechanism that uses two-line element sets (TLES) to predict the object's motion. Observation sessions were usually on the order of 1–2 hours, with longer periods being more favorable (for reasons discussed later in this paper).

Aside from the operator putting the spacecraft in an intentional spin state about its major spin axis (as with TDRS-1[4]), there are several natural effects that influence the rotational motion of the satellite. The major contributors are solar radiation pressure, and gravity-induced torques from the Earth, Moon, and Sun. The magnitude of torques due to solar radiation pressure may be significant depending on the reflectivity of the large apertures that are common on many GEO satellites. While the magnitudes of torques due to gravity may be comparatively smaller[1], the fact that they are constant and uncorrected means that they can contribute significantly to the rotational dynamics of the satellite. Of course, no satellite is a completely rigid body, and the dynamics of the flexible appendages complicates the tumbling motion considerably.

There is a good deal of literature available on using light curves to characterize satellites, although this is often limited to active spacecraft.[7, 9, 1, 5] Schildknect, et al. surveyed debris objects, but focused on the low Earth orbit environment.[13] In 2009, Papushev, Karavaev, and Mishina[12] specifically studied the rotation states of retired satellites near geosynchronous orbit. By choosing the rotation period as the interval between the largest spikes in relative visual magnitude, they found that most of the satellites that they observed had rotation periods ranging from 2–430 seconds. Their results, in general, seem to be in agreement with the large database of ground-based observations known as PPAS—the database of photometric periods of artificial satellites.[7] However, it is of note that three-axis stabilized spacecraft in GEO are a relatively recent advancement, and the bulk of many of these studies consists of spacecraft which were spin-stabilized during their controlled lifetime.[2] Additionally, the measurement between peaks likely does not reflect the reduced full rotational period, and instead is indicative of higher-frequency harmonics. Our observations revealed a repetitive structure in a wider envelope at longer time scales than [12] analyzed, which appear to be the true tumble rate.

Determination of the rotational period of a tumbling spacecraft using only visual magnitude measurements is a difficult problem. In essence, it requires resolving a complex, periodic signal using discrete samples. It is expected that the satellite properties—such as complicated rotational dynamics or the geometry of its reflective surfaces—result in higher-frequency structure, while lower-frequency contributors include observation geometry (as in Fig. 1) and atmospheric effects. In order to reconstruct the high frequency structure in the signal, we must ensure that the sampling period is sufficiently short. Fig. 3 illustrates the problem of discrete sampling: there may be ambiguity in the frequency of the underlying signal. Given a sampling frequency $f_s$ and a set of samples which describe a periodic signal with frequency $f_0$, there is an integer ambiguity such that the same set of samples also describes a signal with frequency $f_0 + kf_s$, where $k \in \mathbb{Z}$.[11] The Nyquist sampling theorem states that the $f_s$ should be twice the frequency of the underlying signal in order to overcome this ambiguity.[11] As our sample rate is typically 1–3 seconds (including integration time and processing), we are able to definitively reconstruct frequencies less than $f_s/2 = 1/6$Hz, corresponding to an attitude rate of 60°/sec, which is well outside the range of expected attitude rates.

Low-frequency structure is more straightforward (though not necessarily easier) to capture: the observation period simply needs to be longer than the rotational period of the satellite. Fig. 4 illustrates the problem: although one may observe what appears to be a full period of a signal, the actual period may be longer. So, if we wish to observe the entire rotational period of a satellite tumbling at 1°/sec, we need to perform at least 360 seconds of observations. Consequently, if we do not see a full period over our observation span $T$, we can deduce that the actual period is therefore greater than $T$, and thus the rotational frequency is less than $1/T$. As our main objective is to place definitive bounds on the maximum tumble rates, this is often sufficient.

The problem of separating effects of satellite geometric features from rotational motion remains. Simply measuring the period between peaks on a visual magnitude curve may be misleading, as the curve may be complex enough to have several similar repeating segments within a single proper period. Even a completely stable satellite may appear to exhibit high-frequency "motion" simply by virtue of slightly changing reflections off of complex reflective surfaces. The changing Sun-spacecraft-observer angle will cause long-periodic effects on the measured relative magnitude. Additionally, the measurements of visual magnitude will inevitably be noisy, further confusing the issue.

[1] Gravity gradient torque depends on the inverse of the cube of distance from the central body.[17]

[2] By one account published in 2000, there was only one retired three-axis satellite available for observation.[9]

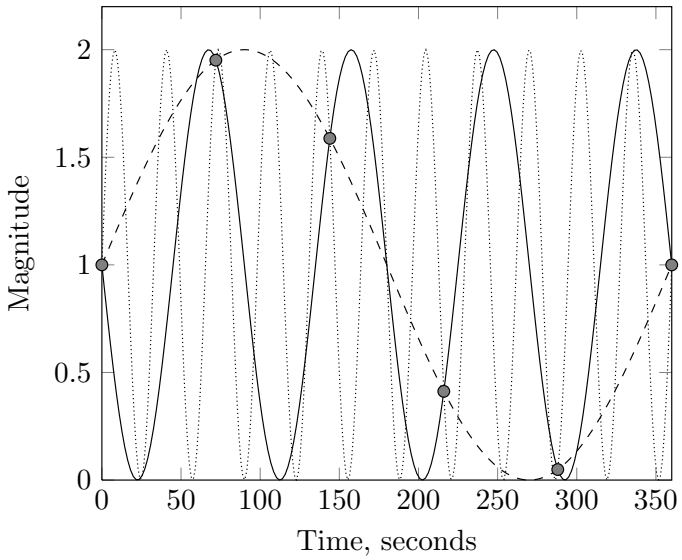


Fig. 3: Illustration of the discrete sampling problem: many different signals fit the discrete samples (grey dots).

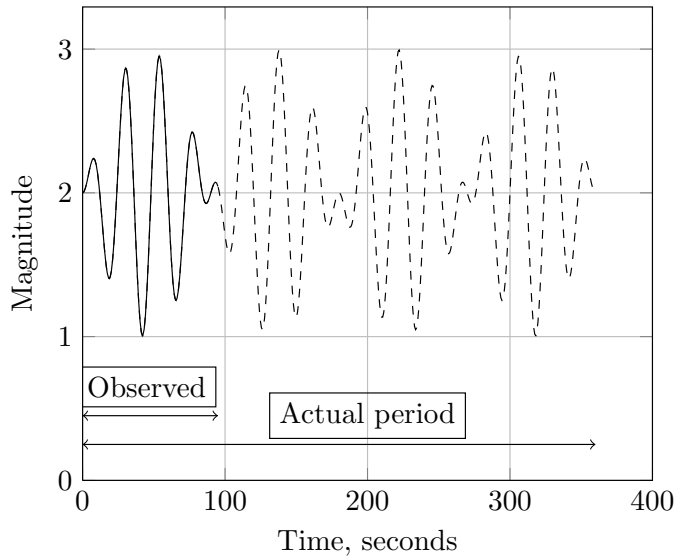


Fig. 4: A complex signal that has an actual period much longer than the observed period.

## 3. METHODOLOGY

Observations for this study were obtained at the NRL's optical research facility located at Midway Research Center near Quantico, VA.[16] It consists of a 1-meter primary mirror Schmidt-Cassegrain telescope mounted in an azimuth/elevation configuration. Measurements were recorded from an SBIG 512×512 pixel charge-coupled device (CCD) using a one-second exposure time and an 8 arcminute field of view.

A typical collection period begins with acquiring the satellite, using predictions generated via publicly-available two line element sets (TLES). After acquisition, the telescope is allowed to track the satellite as it moves across the sky. Prior to actual measurements, "dark frames" are taken with a solid plate blocking the CCD in order to characterize the noise across the sensor. After this, collections begin—session length ranges from 15 minutes to several hours, depending on the relative drift rate of the observed satellite. After the collections are taken, several more dark frames are generated. Finally, calibration frames are collected using the nearest Landolt astrometric standard stars[10] (within 3° of the last satellite collection point). This entire process ensures that the visual magnitude measurements are as close to truth as possible, and allows for some automatic processing, such as removing streaks and noise from the frames in order to isolate the satellite.

Satellites of interest to the Phoenix mission were selected for this survey: retired spacecraft in a super-GEO graveyard orbit. Slight preference was placed on satellites that were three-axis stabilized prior to their retirement. The list was refined based on satellites that were in view of the observatory during the observation campaign, which spanned January–May of 2012. Cloud cover and facility availability further constrained the satellites we were able to observe for a meaningful amount of time.

Some of the initial processing was done in Peranso,[15] a tool that is widely used in the asteroid detection community for working with unresolved observations. It streamlines much of the calibration process, and can perform a Fourier analysis of light curves (FALC) as pioneered by Harris, et al.[8] The success and ubiquity of this method in the asteroid observation realm prompted us to apply it to our problem, and it proved to be a useful tool in our survey. Typically, results were fed into FALC as a first-cut analysis. For objects without a very complex attitude profile, this analysis proved to be sufficient in characterizing the maximum tumble rate.

### 3.1. Novel Analysis Techniques

To reduce possible misinterpretations of the tumble rate, we attempt to modify light curve analysis techniques to reduce background variations and amplify only features in the light curves that repeat at regular intervals in a single pass. This was done as a separate analysis from the Peranso method to both verify the Peranso results and develop techniques better suited to the differences inherent in satellite versus asteroid light curves.

A first step in this process was to mitigate the variation in background levels. To accomplish this, every analysis was preceded by a third order polynomial fit to each light curve, which was then divided into the light curve to normalize the curves and reduce low frequency variations. This method is applicable with satellites since strong spikes in the light curve at frequencies higher than the tumble rate are common. The background normalization does not affect these high frequency spikes and it is repeating patterns of these spikes which then indicate the tumble rate. This is a characteristic that is typically a fundamental difference between satellites and asteroids since asteroids typically do not exhibit these regularly spaced, higher freuqency spikes at frequencies higher than the tumble rate.

Initial attempts used Fourier transforms to look in frequency space and auto-correlations in the time domain. These techniques were seen to sometimes work but often erroneously show the strongest peaks/correlations at frequencies higher than expected for satellites with known tumble rates. Also, for auto-correlations, peaks where correlations were higher were broad, with ill-defined frequencies, resulting in a large uncertainty. In an attempt to improve the identification of true tumble rate, a new technique, dubbed the *cross-residual technique*, was investigated. This technique involves normalizing the light curve as described above, and then subtracting a time offset ($\Delta t$) version of the same light curve from the original curve then squaring and averaging the resulting residuals as shown in Equation 1 for all possible $\Delta t$.

$$R(\Delta t) = \frac{1}{N} \sum_{t=0}^{t_{\max}/2} \left(I(t) - I(t+\Delta t)\right)^2 \text{ for } \Delta t = 0 \text{ to } \frac{t_{\max}}{2} \tag{1}$$

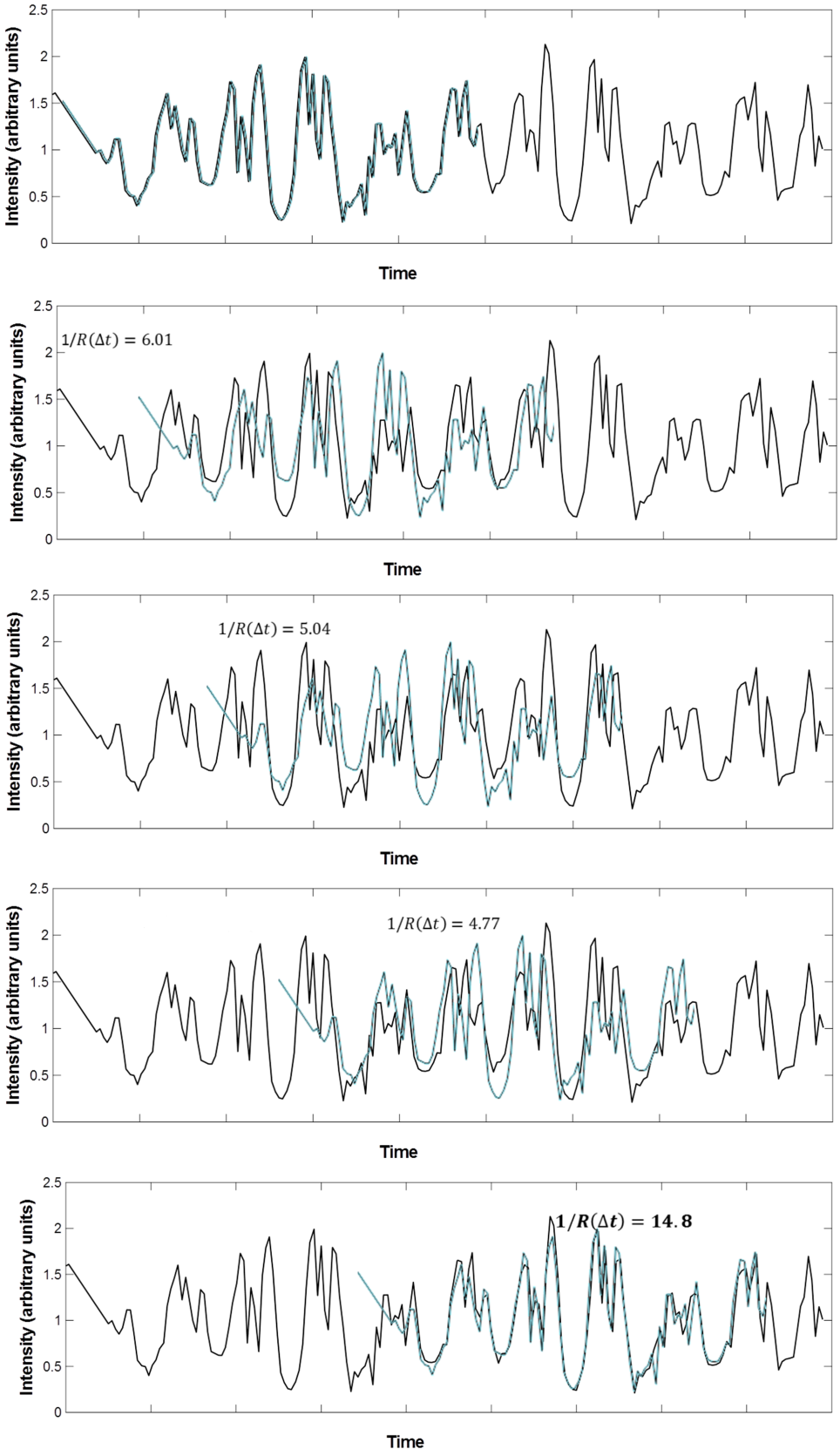


Fig. 5: Illustration of the cross-residuals technique. A higher value of the inverse of the correlation $R(\Delta t)$ is a strong indicator that a repeating pattern has been found, as in the last plot above.

Figure 5 shows an example of this process. For light curves with strong peaks that have a broad envelope that repeats over a longer time, this technique results in the smallest residual where both the repeating peaks and the broad envelope match up. This broad envelope is indicative of a full revolution of the satellite over which the multiple higher frequency glints repeat as the same structures rotate in and out of view. For clarity in plotting, $1/R(\Delta t)$ is plotted to clearly show the strongest peak when both the individual peaks and envelope overlap.

In all the analysis performed, a copy of the same light curve was used to determine the cross-residual. For future work, it is planned to investigate using this technique as a "true" cross-residual where different light curves on different passes of the same satellite are "crossed" using the above formula with intensities $I_1$ and $I_2$ as opposed to $I_1$ and $I_1$. This technique is analogous to an auto-correlation versus a cross-correlation.

Manual inspection of the light curves and incorporation of known characteristics of some satellites were also crucial to the estimation process. The primary aspect of the manual inspection concerns estimating the number of expected brightness spikes (changes of $> 1$ magnitude) from the body, solar panels, or other large features. This allows us to determine differences between observing structural features at higher frequency and full periodic motion of the satellite.

All of these techniques were used together to estimate the most likely upper bound on the tumble rate of each object. For some well-defined light curves, the tumble rate estimates from all sources were in agreement, and there was no ambiguity. However, for some objects, some ambiguity remained; in these cases, all estimates and external data were considered in selecting the most probable maximum tumble rate. The results presented here reflect this thought process.

## 4. RESULTS

A plot of relative magnitude over time is shown for a DirecTV-1 (catalog number 22930) pass in Fig. 7. DirecTV-1 is built around the Hughes Space and Communications Company (now part of Boeing) HS-601 three-axis stabilized satellite bus (pictured in Fig. 6). This particular session was nearly an hour long, making it more likely that we see a full rotation. Indeed, the curve has a definitive structure, with variations of more than one order of magnitude, and it is quite clear that we see multiple full revolutions. However, the problem of distinguishing between harmonics remains.

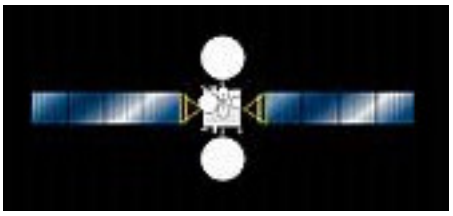

Fig. 6: HS-601 satellite bus (from `http://www.boeing.com/assets/images/defense-space/space/bss/factsheets/601/601sats/dtv1r_n.jpg`).

Figure 8 shows the results of the cross-residual analysis for this particular light curve. The presence of several relatively strong peaks indicates that more analysis is required to make a definitive call. Using the assumption that each peak in the light curve represents a major structural element of the spacecraft (e.g. one of the faces of the bus) and counting peaks, we can pick out the most likely full rotational period as 10.9 minutes, corresponding to a rate of 0.55°/sec.

Fig. 10 shows the relative magnitude measurements Superbird A1 (catalog number 22253). It is built around an LS-1300 three-axis stabilized bus (built by Space Systems/Loral, and pictured in Fig. 9), and few details could be found concerning its retirement. The structure of this light curve is much more complicated: there are several well-defined peaks, but a definitive, measurable primary period is somewhat difficult to pick out. This is a case that embodies the issues discussed in Section 2, and requires synthesized analysis from multiple sources to properly characterize. From Fig. 10, it appears we observe a full rotational period over approximately 50 minutes (in the middle section), measured by inspection.

By applying the cross-residuals method to this, we see some persistent ambiguity. While the strongest peak is near 58.3 minutes, there is also a significant peak at 46.1 minutes. Because our objective is to find

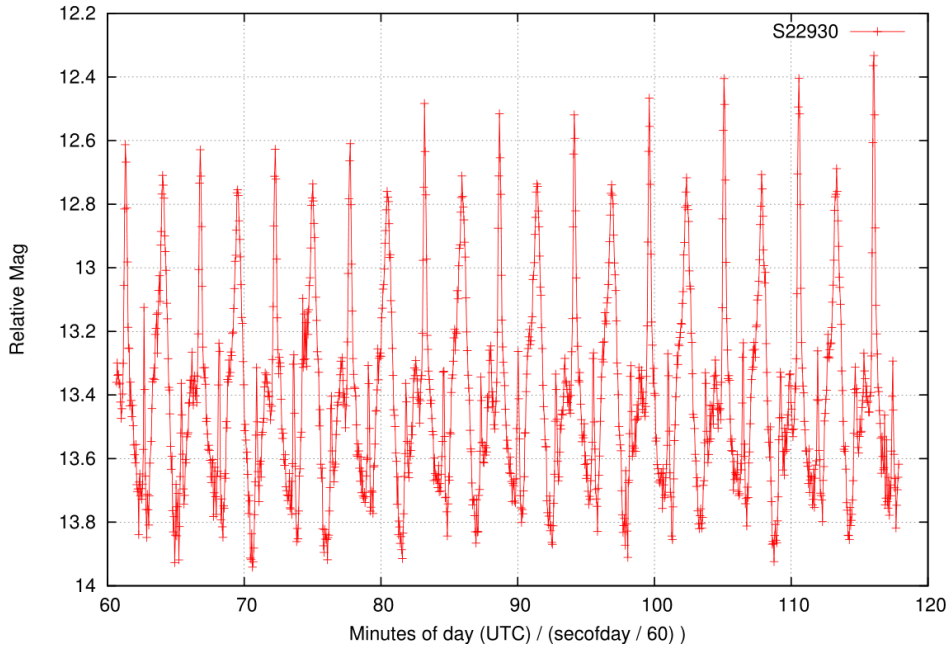


Fig. 7: Plot of relative magnitude for DirecTV-1.

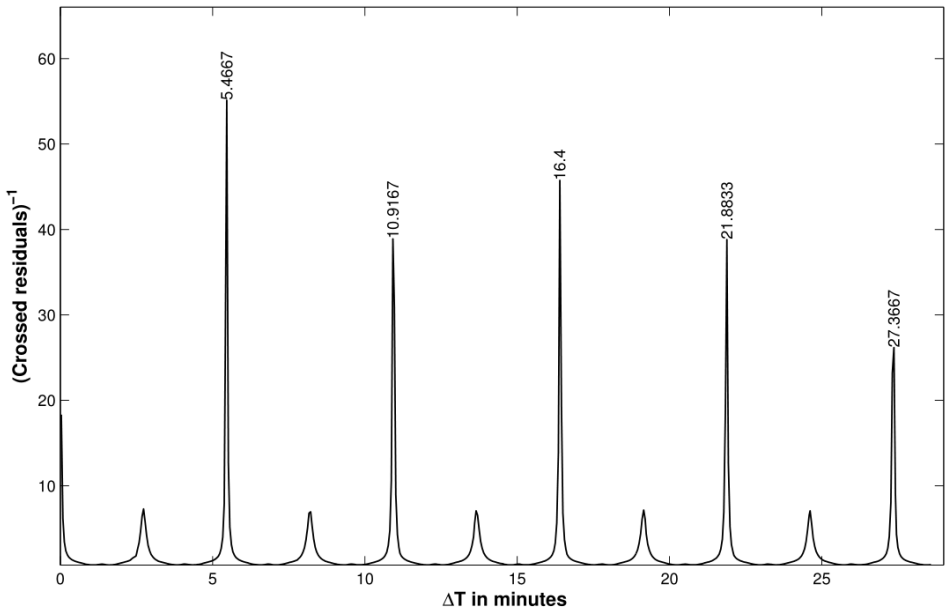


Fig. 8: DirecTV-1 rotational periods resulting from cross-residual analysis.

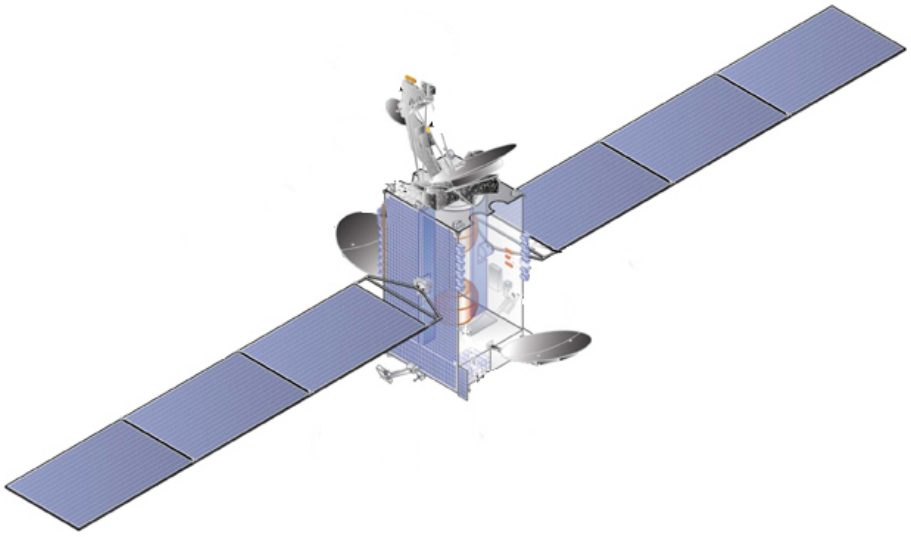

Fig. 9: LS-1300 satellite bus (from `http://sslmda.com/images/aboutssl/1300overview.jpg`).

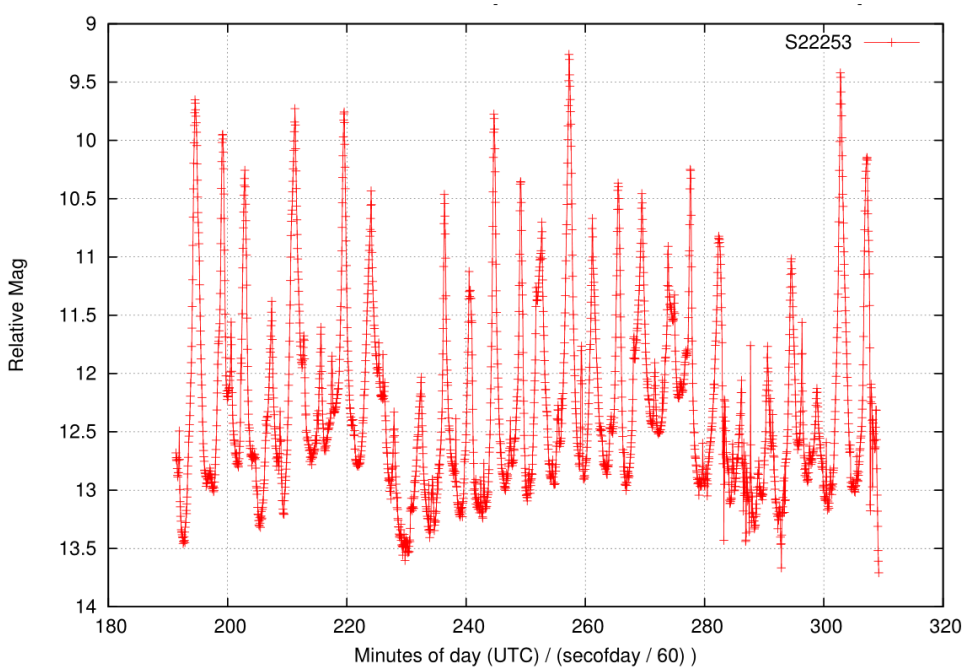


Fig. 10: Relative magnitude plot for Superbird A1, showing much more complex behavior.

the upper bound on rotational rate, we choose the faster (46.1 minute) period. The results of this analysis are plotted in Fig. 11.

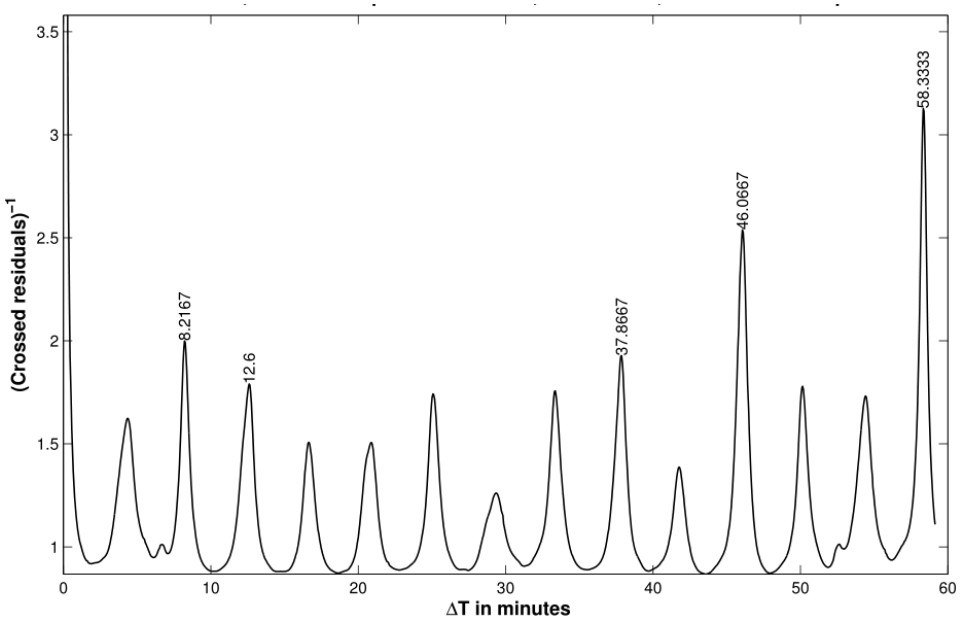


Fig. 11: Superbird A1 rotational periods resulting from cross-residuals analysis.

Intelsat 705 (catalog number 23528) is, like Superbird A1, an LS-1300 stabilized bus. Launched in 1995, it was retired in 2011. Details such as passivation procedures, etc. could not be found, although the TLES indicate it was placed in a super-synchronous disposal orbit. Fig. 12 shows the extracted light curve from one collection period, and Fig. 13 shows the result of the cross-residuals analysis. The cross-residuals analysis for this satellite showed a consistent, strong peak near 14 minutes, corresponding to a rotation rate of 0.43°/sec. However, Fig. 12 does not appear to show an obvious full rotation, indicating that the cross-residuals analysis simply may not have enough data to make an accurate estimate. As in other cases, we report the estimate as an upper bound, with the expectation that the actual rate is significantly slower.

Tracking and Data Relay Satellite-1 (TDRS-1) (catalog number 13969) is a three-axis stabilized satellite that began the retirement process in 2009. As part of the passivation/disposal process a spin rate of 0.5°/sec was induced about its $Z$ axis (parallel to the main antenna pointing axis).[4][3] Although there is noise evident in the measurements, a clear periodic structure is present. However, this structure is misleading. In fact, the magnitude of the oscillations is quite small, indicating that we are simply viewing reflections off of different features of the bus, which is pictured in Fig. 14. Any resulting estimate will need to be framed with this context. Figures 15 to 18 show the light curves from different observing sessions. The same high-frequency, low-amplitude structure is visible in all cases. Only Figures 17 and 18 show any large-magnitude changes, indicating that we observed part of a full rotation during these periods (e.g. a single bus face or solar panel). Nevertheless, by inspection, a minimum period of 7–9 minutes (corresponding to 0.857–0.667°/sec) is found, with the understanding that the true rate is likely significantly lower.

[3] [4] also includes a very thorough discussion of the dynamics involved in the passivation process.

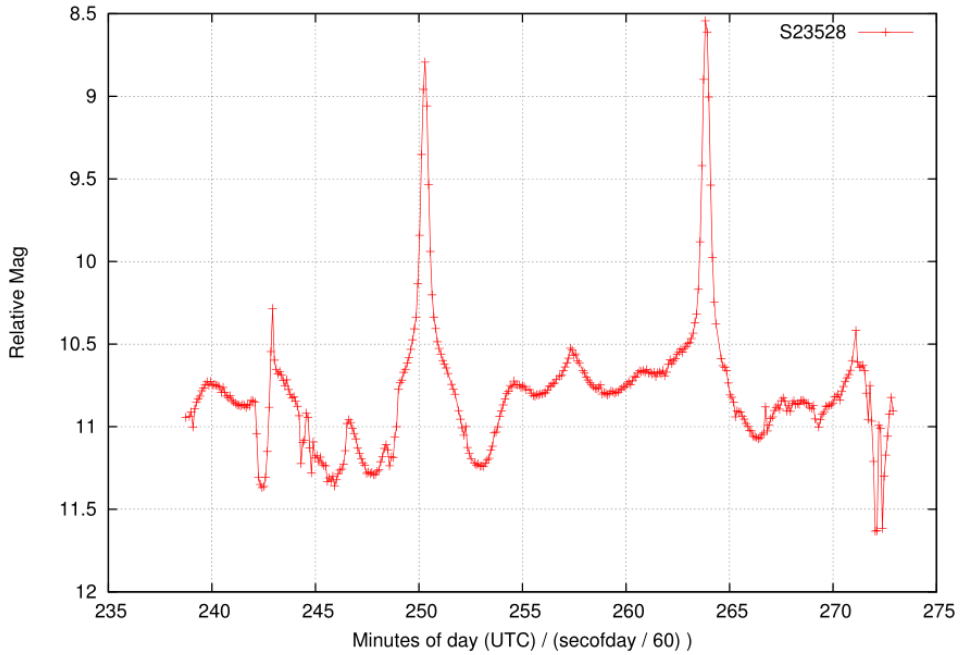


Fig. 12: Relative magnitude plot for Intelsat 705.

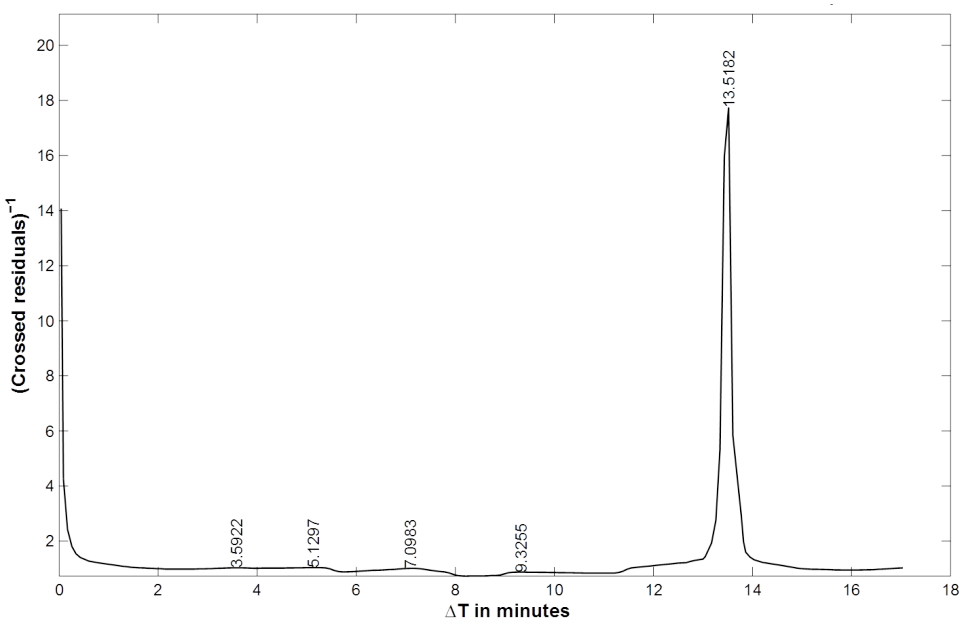


Fig. 13: Intelsat 705 rotational periods resulting from cross-residuals analysis.

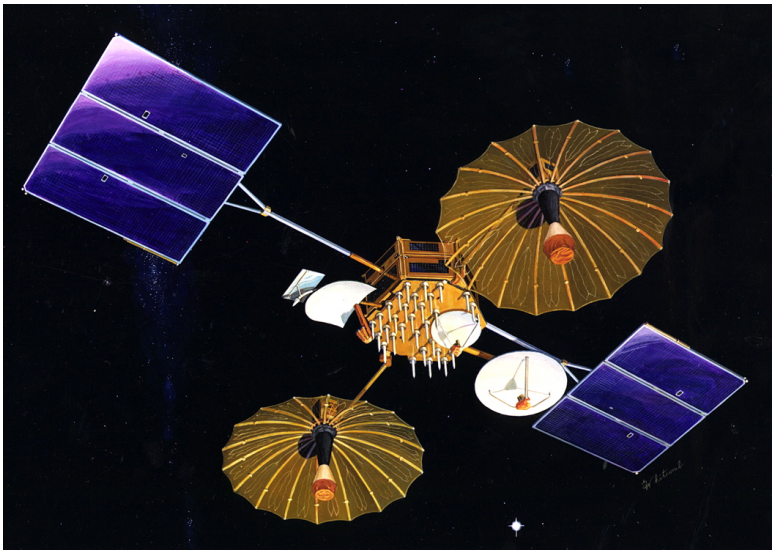

Fig. 14: Artist's rendition of a first-generation TDRS satellite on-orbit. (From `http://www.nasa.gov/content/tracking-and-data-relay-satellite-tdrs/`)

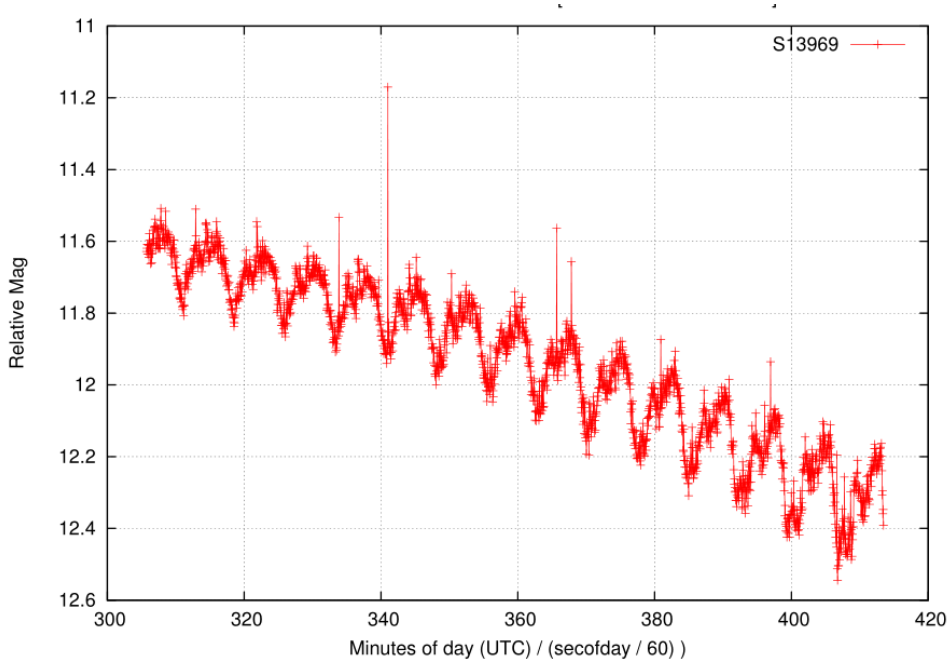


Fig. 15: Plot showing relative magnitude over approximately 2 hours for the retired TDRS-1 satellite.

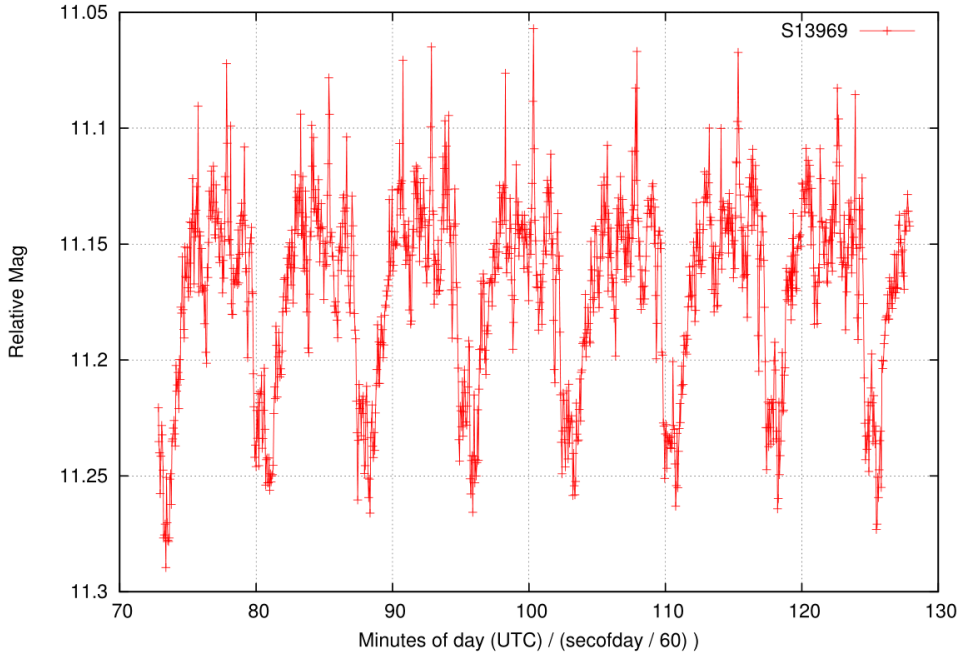


Fig. 16: Plot showing relative magnitude over approximately 60 minutes for the retired TDRS-1 satellite.

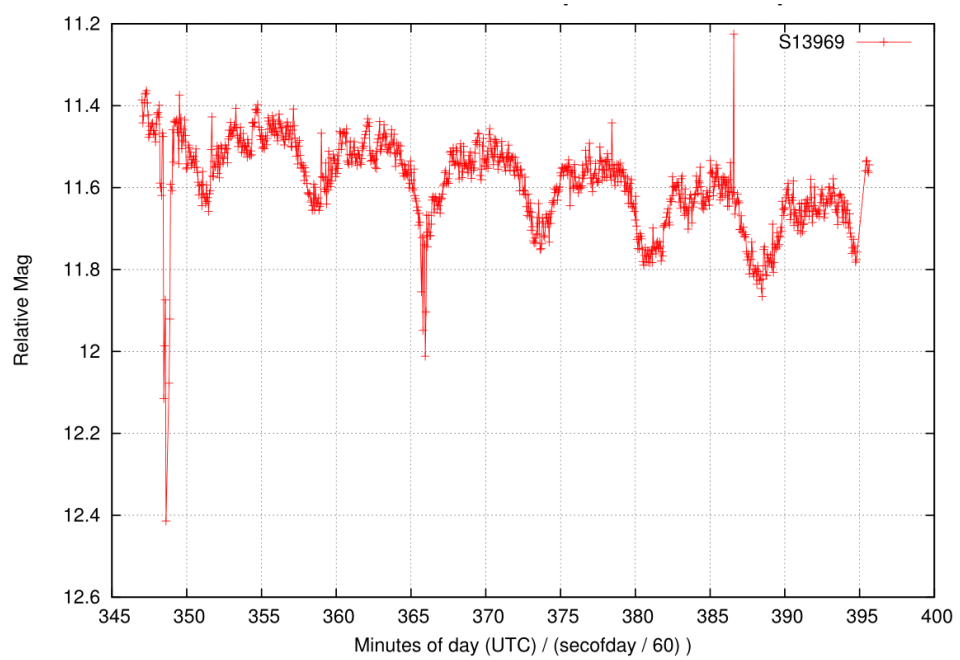


Fig. 17: Plot showing relative magnitude over approximately 50 minutes for the retired TDRS-1 satellite.

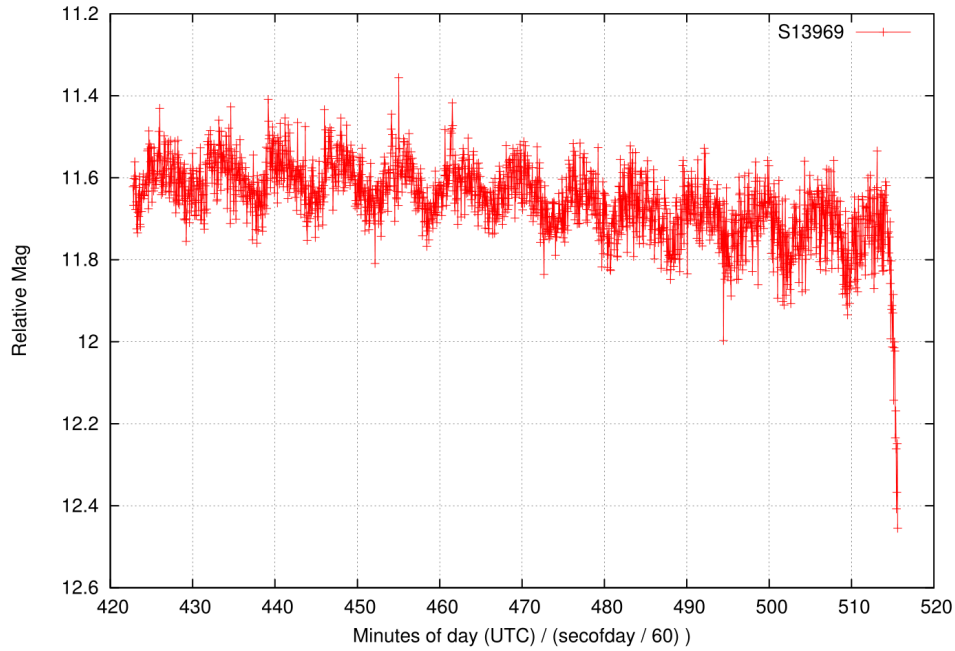


Fig. 18: Plot showing relative magnitude over approximately 90 minutes for the retired TDRS-1 satellite.

### 4.1. Validation

The rate determination process was validated using observations of a U.S. spacecraft with attitude control. Release approval for specific technical data was not obtainable from the government owner. The relative magnitude plot is shown in Fig. 19, and the cross-residuals plot is shown in Fig. 20. There exist several harmonic frequencies of similar strengths, but by incorporating prior knowledge of the spacecraft's structural characteristics, the correct frequency is readily apparent from the cross residuals plot. Over four separate observation sessions, the estimated rates from FALC and the cross-residuals analysis matched the rate from telemetry to within 0.59%–1.12%.

A histogram summarizing the results of this survey is presented in Fig. 21, and the results are tabulated in Table 1. As the Phoenix mission is most interested in an upper limit of the tumble rate that should be expected (for reasons discussed in Section 2), focus was placed on determining this limit, and not necessarily separating out higher-frequency effects. Indeed, in several cases, more observations (perhaps throughout the year, at varying observation geometries) will be required for a more precise determination of the actual rates present. As the Fig. shows, a vast majority of the satellites surveyed are tumbling below 1°/sec. This is not meant to be an exhaustive survey of all retired GEO satellites—indeed, our sample is biased in that three-axis stabilized buses were of higher interest to the Phoenix program.

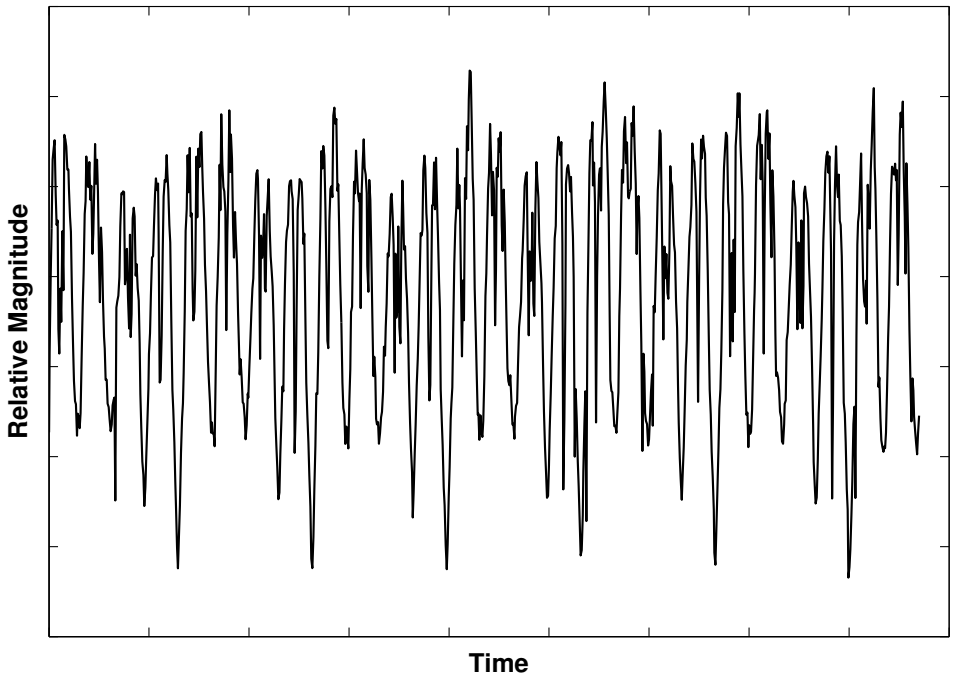


Fig. 19: Relative magnitude plot for government reference spacecraft.

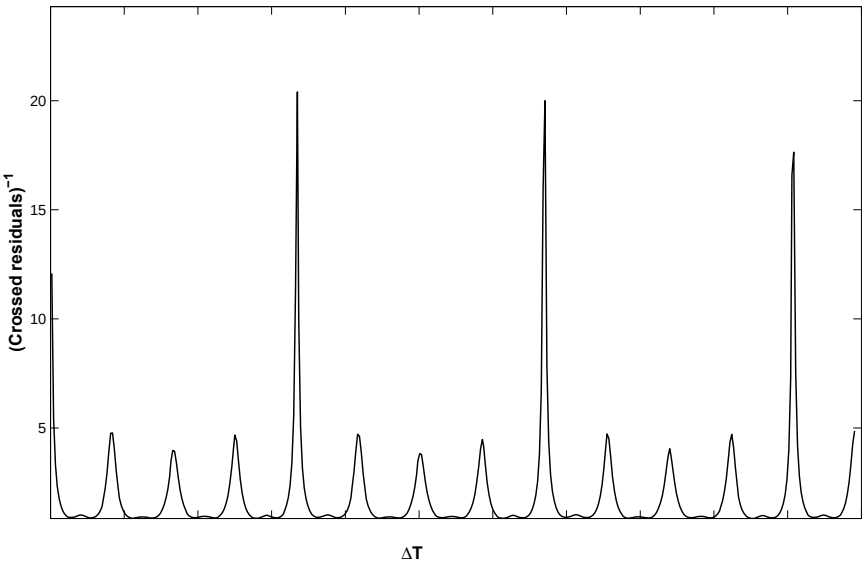


Fig. 20: Cross-residual analysis for government reference spacecraft.

Table 1: Tabulated results of the survey.

| Satellite Name (Cat. No.) | # of Collections > 30 min. | Max. Tumble Rate [°/ sec] |
|---|---|---|
| Galaxy 10R (26056) | 7 | 0.14 |
| Superbird A1 (22253) | 6 | 0.13 |
| TDRS-1 (13969) | 5 | 0.80 |
| Thuraya 1 (26578) | 10 | 0.25 |
| Superbird B1 (21893) | 2 | 0.10 |
| DirecTV 1 (22930) | 2 | 0.55 |
| Echostar V (25913) | 3 | 0.40 |
| Intelsat 605 (21653) | 1 | 2.10 |
| Intelsat 705 (23528) | 1 | 0.43 |
| Bsat 1A (24769) | 1 | 0.41 |
| Superbird A (20040) | 3 | 0.86 |
| DirecTV 3 (23598) | 1 | 0.39 |
| Intelsat 604 (20667) | 1 | 2.60 |
| SATCOM C5 (13631) | 0 | 0.45 |
| Intelsat 802 (24846) | 1 | 0.47 |
| Intelsat 704 (23461) | 4 | 0.27 |
| Sirius 2 (25049) | 1 | 0.20 |
| Intelsat 2 (23175) | 0 | 0.44 |
| TDRS-4 (19883) | 1 | 0.06 |

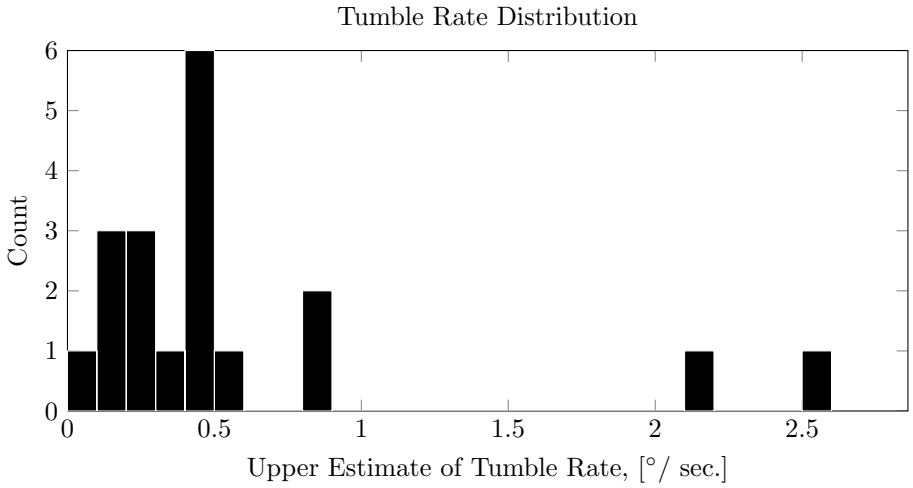


Fig. 21: Histogram of results of this survey.

## 5. FUTURE WORK

As the focus of this work was on finding bounding upper rates for these objects, less emphasis was placed on separating out and attributing higher-frequency harmonics. Further analysis is required for these more precise estimates, including longer observation periods and varying observation geometries (by observing at different times throughout the year). Additionally, spectral analysis of the reflected light could help separate out different features, such as solar arrays. Modeling and simulation of the full rotational state of an example spacecraft could also be leveraged to provide a level of verification for these techniques.

## 6. SUMMARY

The Naval Research Laboratory's telescope at Midway Research Center was used to collect photometric data from a number of retired GEO assets. In order to account for several complicating factors, including rapidly changing Sun-spacecraft-observer angles and complex spacecraft geometry, several methods were used to estimate the tumble rate of these objects. The most basic analysis involved simple inspection of the normalized relative magnitude curves. Typically, a more advanced analysis was required, and here we used Fourier analysis of light curves (FALC) and the novel cross-residuals method, both of which extract frequency information from a complex signal. To bolster confidence in our methodology, the same analyses were performed using photometric measurements of a known asset near GEO over several observing sessions. When compared with the attitude rate from telemetry, the analysis agreed to within approximately 1%.

All data and analysis sources were considered for determining the most probable maximum tumble rate, and often these sources were in close agreement. In particular, the cross-residuals method presented here performed quite well in identifying and discriminating primary rotation periods from their harmonics. The results show that the majority of objects we observed are tumbling well below the notional 1°/sec rate considered favorable for the Phoenix program. This is a promising result in regard to the serviceability of retired GEO assets.

## DISCLAIMER

The views expressed are those of the authors and do not reflect the official policy or position of the Department of Defense or the U.S. Government.

## REFERENCES


[1] C. M. Alcala and J. H. Brown. Space object characterization using time-frequency analysis of multi-spectral measurements from the Magdalena Ridge observatory. In *Proceedings of the Advanced Maui Optical and Space Surveillance Technologies (AMOS) Conference*, 2009.

[2] D. Barnhart, L. Hill, M. Turnbull, and P. Will. Changing satellite morphology through cellularization. In *Proceedings of the AIAA Space Conference 2012*, 2012.

[3] D. Barnhart, B. Sullivan, R. Hunter, J. Bruhn, E. Fowler, L. Hoag, S. Chappie, G. Henshaw, B. Kelm, T. Kennedy, M. Mook, and K. Vincent. Phoenix program status 2013. In *Proceedings of the AIAA Space Conference*, 2013.

[4] C. A. Benet, H. Hoffman, T. E. Williams, D. Olney, and R. Zalesky. Attitude control and orbital dynamics challenges of removing the first 3-axis stabilized tracking and data relay satellite from the geostationary arc. In *Astrodynamics 2011*, volume 142 of *Advances in the Astronautical Sciences*, San Diego, CA, 2011. Univelt, Inc. AAS 11-593.

[5] M. Bolden, P. Sydney, and P. Kervin. Pan-STARRRS status and GEO observation results. In *Proceedings of the Advanced Maui Optical and Space Surveillance Technologies (AMOS) Conference*, 2011.

[6] A. B. Bosse, W. J. Barnds, M. A. Brown, N. G. Creamer, A. Feerst, C. G. Henshaw, A. S. Hope, B. E. Kelm, P. A. Klein, F. Pipitone, B. E. Plourde, and B. P. Whalen. SUMO: spacecraft for the universal modification of orbits. volume 5419, pages 36–46, 2004.

[7] B. De Pontieu. Database of photometric periods of artificial satellites. *Advances in Space Research*, 19(2):229–232, 1997.

[8] A. Harris, J. Young, E. Bowell, L. Martin, R. Millis, M. Poutanen, F. Scaltriti, V. Zappal, H. Schober, H. Debehogne, and K. Zeigler. Photoelectric observations of asteroids 3, 24, 60, 261, and 863. *Icarus*, 77(1):171–186, 1989.

[9] R. Lambour, R. Bergemann, C. von Braun, and E. M. Gaposchkin. Space-based visible space object photometry: initial results. *Journal of Guidance, Control, and Dynamics*, 23(1):159–164, 2000.

[10] A. U. Landolt. Broadband UBVRI photometry of the Baldwin-Stone southern hemisphere spectrophotometric standards. *The Astronomical Journal*, 104:372–376, 1992.

[11] R. G. Lyons. *Understanding Digital Signal Processing*. Prentice Hall, 3rd edition, 2010.

[12] P. Papushev, Y. Karavaev, and M. Mishina. Investigations of the evolution of optical characteristics and dynamics of proper rotation of uncontrolled geostationary artificial satellites. *Advances in Space Research*, 43:1416–1422, 2009. doi:10.1016/j.asr.2009.02.007.

[13] T. Schildknect, U. Hugentobler, and A. Verdun. Optical observations of space debris with the Zimmerwald 1-meter telescope. *Advances in Space Research*, 19(2):221–228, 1997.

[14] B. Sullivan, D. Barnhart, L. Hill, P. Oppenheimer, B. L. Benedict, G. Van Ommering, L. Chappell, J. Ratti, and P. Will. DARPA Phoenix payload orbital delivery (POD) system :"FedEx to GEO". In *Proceedings of the AIAA Space Conference*, 2013.

[15] T. Vanumnster. Peranso period analysis software. `http://tonnyvanmunster.ipage.com/peranso/index.htm`, 2007. Accessed 29 April, 2013.

[16] M. Vilcheck, A. Reed, A. Peltzer, M. Davis, and H. R. Burris. Overview of the NCST's new optical research facility. In *Aerospace Conference, 2001, IEEE Proceedings.*, volume 3, pages 3/1489–3/1494 vol.3, 2001. doi:10.1109/AERO.2001.931379.

[17] J. R. Wertz and W. J. Larson, editors. *Space Mission Analysis and Design*. Microcosm Press, Hawthorne, CA, 3rd edition, 1999.